J Ther Eng, Vol. 10, No. 3, pp. 670−679, May, 2024

Journal of Thermal Engineering
Web page info: https://jten.yildiz.edu.tr
DOI: 10.14744/thermal.0000821

Research Article

Numerical simulation of the shell cooling of a rotary kiln

Bouhafs MOHAMMED[1,*], Meghdir ABED[1], Bouchentouf Ikram MIMOUNA[1]

[1]*Institute of Maintenance and Industrial Safety, University of Oran 2 Mohamed Ben Ahmed, Oran, J9RM+MRG, Algeria*

ARTICLE INFO

Article history
Received: 24 February 2023
Revised: 31 May 2023
Accepted: 01 June 2023

Keywords:
Efficiency; Fins; Heat Transfer; Rotary Kiln; Shell; Temperature Distribution

ABSTRACT

The rotary kiln is considered the heart of cement manufacturing plants, so any malfunction can lead to significant losses for the company. These equipment's are exposed to very high thermal stresses through the three modes of heat transfer, conduction, convection, and radiation. They are also subject to very important mechanical stresses at the level of the drum shell, the tires, the mass of refractory bricks, and the formation of the crust inside the kiln during start-up. The temperature of the flame is around 2000 °C, that of the internal material of the kiln can exceed 1450 °C, and the external temperature of the drum shell can reach 500 °C, particularly in the burning zone. These temperatures can lead to elastic and even plastic deformations. The aim of our study is to numerically simulate the cooling of the drum shell, in its burning zone over a length of 17 m, by placing 72 square-shaped fins on its external surface. This study is a continuation of another one that has already been published [1]. The numerical method used is the finite element method as implemented in the ANSYS Workbench calculation code. The results presented are based on the distribution of the external temperature of the drum shell in the burning zone for different cases. The results obtained show a decrease in the external temperature of the drum shell of about 40% in the case of a drum shell equipped with fins compared to one without fins.

Cite this article as: Mohammed B, Abed M, Mimouna BI. Numerical simulation of the shell cooling of a rotary kiln. J Ther Eng 2024;10(3):670−679.

INTRODUCTION

The rotary kiln is considered to be the heart of a cement plant, for the production of clinker. It is subjected to very high thermal and mechanical loads. The temperature of the material inside the oven can reach 1500°C and that of the flame exceeds 2000°C, which can cause a certain number of problems on all the parts of this equipment. Among these organs, we have the shell of the furnace which is made of cylindrical steel sheet. This is the part that can suffer from damage such as red spots (hot spot), elastic and even plastic deformations. Our work is based on the study of heat transfer in the kiln, in order to find how to reduce the temperature of the shell. Research works has focused on the problem, among which we will cite those of Shvachko et al. [2] who present a method for increasing the efficiency of rotary kilns by varying the thickness of the crust, considered to insulate and allow the conservation heat. A. Gallo, et al. [3] developed a laboratory-scale rotary kiln and tested it using a

***Corresponding author.**
*E-mail address: mohamedbouhafs@yahoo.fr, bouhafs.mohamed@univ-oran2.dz

This paper was recommended for publication in revised form by Editor-in-Chief Ahmet Selim Dalkılıç

Published by Yıldız Technical University Press, İstanbul, Turkey

solar simulator. The numerical results showed a good agreement with the experimental data, so the thermal losses could be quantified in detail. Wirtz et al. [4], make a study which consists in estimating the crusting layer in the rotary kiln in order to control the temperature of the shell. This temperature is introduced into a heat transfer model, in order to deduce the thickness of this layer. Rindang et al. [5] conducted an experimental study to deduce a heat and mass transfer model within a rotary dryer, by varying the air injection velocity and the drying temperature. C. Gu et al. [6] proposed a mathematical model of heat and mass transfer, in order to study the drying characteristics of biomass particles. The simulation results indicated that the drum temperature can have a significant influence on the drying behaviors of the particles. Bongo Njeng et al. [7] develop a model based on dimensional analysis for the calculation of the wall-material heat transfer coefficient for heating temperatures varying from 100 to 500°C, while considering the service conditions. Mirhosseini et al. [8] studied the effect of an absorber in the form of an arc placed around the rotary kiln, in order to permit the recovery of a part of this quantity of heat dissipated by the rotary kiln for use in d other applications. K. Wang et al. [9] experimentally and numerically studied a new heat exchanger using batteries of tubes arranged in a certain orientation. The numerical results indicate that these batteries of tubes are more efficient when they are arranged in a certain orientation. Yin et al. [10] propose a system for recovering waste heat from a rotary kiln by establishing mathematical relationships linking the heat transfer zones in the kiln to the mass flow rates of the recovery exchangers. Ramanenka et al. [11], models a hot rotary kiln lined with three types of bricks, using the finite element method. They studied the reliability of this modeling, by highlighting the level of tensile stress that can potentially occur. Qian Yin et al. [12] carried out an experimental work which consists of the design of a system for recovering the heat lost by a rotary kiln. It is designed with nine heat exchangers for heating the water. This design is mathematically modeled taking into account the exchange surface, the total energy, the regenerated entropy and the temperatures of the fluids. Agrawal et al. [13] present a modeling of the heat transfer of convection, radiation and conduction between the hot gas and the surface of the refractory wall. Steady-state finite differences are assumed. Parametric analysis of humidity rate, material flow, gas flow, angle of inclination and rotational velocity of the kiln are made. M. Csernyei et al. [14] described the process used for the numerical analysis of convective heat transfer from multiple large jets. The inclusion of forced convection in the kiln resistance model resulted in a decrease in shell temperature compared to free convection. Yin et al. [15] present a mathematical model to analyze shell temperatures and heat loss rates in different regions of the rotary kiln. They established a heat exchange surface optimization model to describe the relationship between the design parameters and the mass flow rate of each heat exchanger. Shahin et al. [16] developed a mathematical model of energy balance equations including coupled mechanisms of heat transfer and chemical reaction. This should allow thermal energy analysis for lime production. Ustaoglu et al. [17] perform an energy and exergy performance analysis of a wet rotary kiln was performed based on actual data. The results showed that a large amount of thermal energy is discharged from the kiln chimney. Csernyei [18] highlights through a numerical simulation, the heat transfer by forced convection resulting from the jets oriented on the shell of a rotary kiln, which allows to deduce a correlation representing the cooling of the kiln. Liu et al. [19] numerically simulated the two-dimensional dynamic and thermal behavior between matter and hot gases, on a cross-section inside a rotary kiln. This work has been validated by experimental data. Goshayeshi and Poor [20] have established a complete model of the kiln in order to reduce its energy consumption during the production of cement, taking into account the parameters having a great influence, such as the change in the temperature of the coating, the phase change of the material and the temperature of the combustion gases. Gaurav and Khanam [21] simulated different closure models on a rotary kiln, in order to be able to determine and optimize the temperature profiles of the gas and the material. The input parameters of this simulation are the angle of inclination, the number of rotations of the kiln and the mass flow. Csernyei and Straatman [22], the importance of their study lies in the heat transfer by convection allowing the cooling of rotary cement kilns using large axial fans. From this work, a numerical model was highlighted using turbulence models. Goshayeshi and Poor [23] carried out a simulation in order to know the behavior of the operating parameters of the rotary kiln, namely, the phase change of the material, the temperature of the gas and the internal coating of the kiln. Moussi et al. [24] model a rotary kiln in a dry process cement plant. This simulation resides in the coupling between the mass balance equations and the heat transfer equation. This model is validated by experimental measurements permitting to obtain the temperature, the compositions of the gas and the material along the different zones of the kiln. Luo et al. [25] proposed waste heat recovery thermoelectric generating units to reduce heat losses from rotary kilns. The simulation results show more than 32.85% of waste heat is saved from the kiln surface. Atmaca and Yumrutas [26] show the effects of refractory bricks and the formation of a crust layer on the specific energy consumption of a rotary kiln through a numerical simulation. This allows the energy balance of the system to be calculated. Ariyaratne et al. [27] present a three-dimensional modeling carried out on a cement rotary kiln with a multi-channel air vortex burner, and at high impulse for the combustion of coal as well as for the combustion of animal meal. Yi et al. [28] numerically process

the mathematical model of the heat transfer of an alumina rotary kiln to predict the gas and material temperature profiles in the axial direction. A.C. Caputo et al. [29] proposed the possibility of recovering the radiant heat lost through the furnace surface by a set of pressurized water transport tubes arranged in a longitudinal plane on the surface of a coaxial cylindrical outer shell with the rotary kiln. S. B. Paramane and Sharma [30] have numerically studied the free flow and the heat transfer by forced convection through a rotating cylinder for Re numbers from 20 to 160. They found that the rotation of the cylinder allows the reduction of the number of Nu. I. A. S. Larsson et al. [31] have studied the rotary kiln process numerically and the results obtained show that in steady state they can be used to gain insight into the main characteristics of the flow field. The purpose of the numerical study of G. Krishnayatra et al. [32], is to know the effect of the dimensions, the number and the material of the fins installed on a cylinder on the heat transfer during a natural convection with a constant Rayleigh number. S. K. Rout et al. [33] presents in this work, the effects of the height, the width and the number of fins on the improvement of the heat transfer with the variation of the Nusselt number, the friction factor and the Reynolds number. T. Bano and Ali [34] presents a modeling of heat transfer by condensation on smooth horizontal tubular surfaces with fins, which focuses on three-dimensional (3D) geometric effects, fin density, fin spacing and thickness. S. Mohamad et al. [35], the main objective of their study is to evaluate the entropy production and estimate the cooling time of the furnace. A simulation was carried out to calculate the free convection of the blast furnace with respect to the variation of its cross-sectional area. S. Mohamad et al. [36] present a numerical solution of the continuity, momentum and energy equations for a fluid domain surrounding the outer cylindrical surface of a vertical cylinder with the specific longitudinal section using ANSYS FLUENT 18. The main parameters of this study are the cylinder length, diameter, Rayleigh number, and surface temperature of the cylinder. S. Kumar Rout et al. [37] in their work, the wall temperature of a tube provided with internal fins has been calculated numerically for different numbers, heights and shapes of fins through the resolution of the equations of conservation of mass, momentum and energy in using Fluent. F. Mebarek-Oudina et al. [38], in their study the effects of the Richardson number and the Reynolds number ratio are demonstrated through the numerical study of mixed convection inside a horizontal rectangular pipe combined with an open trapezoidal cavity and heated using two heat sources.

The main objective of our work is to represent the temperature profile of the rotary kiln shell. Our novelty lies in adding fins to the external surface of the kiln shell in its burning zone, and examining the impact of the fins on the temperature profile compared to the kiln shell without fins.

DESCRIPTION OF THE PROBLEM

The rotary kiln is subjected to high temperatures, which poses a problem of damage to the shell. In this work, we carried out a numerical simulation of the thermal behavior of the shell of the rotary kiln in the firing zone of the cement plant. The purpose of this study is to deduce the distribution of the outside temperature of the shell of the cooking zone for two distinct cases. The first case is, the study of the evolution of the external temperature of the kiln in the cooking zone, with a smooth shell as it exists in industry. In the second case, the outer surface of the shell is equipped with fins. Figure 1 gives us a vision of the rotary kiln in our site, where our study was carried out. The dimensions of this kiln are shown in Table 1.

The study was carried out on the cooking zone of the 17 m long rotary kiln. This part is considered to be the most thermally stressed. The outside temperatures in this area often exceed 400°C, and as the shell of the furnace is made of A42 steel, this can lead to elastic and even plastic deformations.

Figure 1. Rotary kiln.

Table 1. The dimensions of the rotary kiln

Kiln dimensions	Value
Total kiln length	80 m
Length of the baking part of kiln	17 m
Inner diameter of the shell	5 m
Shell thickness	30 mm
Refractory brick thickness	220 mm
Kiln litl	2.29°
Number of support	3

Table 2. The constants values of the SST model

α^*_∞	α_∞	β^*_∞	R_β	Mt_0	α_1	$\beta_{i,1}$	$\beta_{i,2}$	$\sigma_{k,1}$	$\sigma_{k,2}$	$\sigma_{\omega,1}$	$\sigma_{\omega,2}$
1	0.52	0.09	8	0.25	0.31	0.075	0.0828	1.176	1	2	1.168

Mathematical Model

Our study consists of an approach of a flow around a horizontal cylinder with a wall at high temperature. For this, it is necessary to quote the adequate formulation for this case. The resolution of the equations governing this flow is done by the K-ω-SST model of the ANSYS-CFX code, the comparison of the results of which constitutes the essential objective of this work. By adopting the SST model simulates the heat transfer of this flow. The Navier Stocks equations [39,40] considered for this incompressible fluid are:

$$\frac{\partial U_j}{\partial x_j} = 0 \tag{1}$$

Momentum Transport Equations

$$\rho U_j \frac{\partial}{\partial x_j}(U_i) = -\frac{\partial P}{\partial x_j} + \mu \frac{\partial^2 u_i}{\partial x_j^2} + \underbrace{\frac{\partial}{\partial x_j}\left(-\rho\overline{u_i' u_j'}\right)}_{\text{Contraintes de Reynolds}} + \rho g_i \tag{2}$$

Energy equation

$$\frac{\partial}{\partial x_j}\left(\rho U_j T\right) = \frac{\lambda}{C_p}\frac{\partial^2 T}{\partial x_j^2} + \frac{\partial}{\partial x_j}\left(-\overline{\rho\, u_j' t_p'}\right) \tag{3}$$

All these equations can be written in the following general form:

$$\underbrace{\frac{\partial(\rho U_j \phi)}{\partial x_j}}_{1} = \underbrace{\frac{\partial}{\partial x_j}\left(\Gamma_\phi \frac{\partial \phi}{\partial x}\right)}_{2} + \underbrace{S_\phi}_{3} \tag{4}$$

Term 1 : transport of ϕ by convection.

Term 2 : transport of ϕ by diffusion.

Term 3 : local production of ϕ.

The *SST* model has a form similar to the standard k–ω model [40]

$$\frac{\delta}{\delta x_i}(\rho k u_i) = \frac{\delta}{\delta x_j}\left[\Gamma_k \frac{\delta k}{\delta x_j}\right] + G_k - y_k + S_k \tag{5}$$

$$\frac{\delta}{\delta x_i}(\rho \omega u_i) = \frac{\delta}{\delta x_j}\left[\Gamma_\omega \frac{\delta \omega}{\delta x_j}\right] + G_\omega - y_\omega + D_\omega + S_\omega \tag{6}$$

Avec $G_k = -\rho\overline{u_i' u_j'}\frac{\partial u_i}{\partial x_i}$, $G_\omega = \alpha\frac{\omega}{k}G_k$: le terme de production de k, ω respectively.

The effective diffusivities for the SST model are given by:

$$\Gamma_k = \mu + \frac{\pi_t}{\sigma_k} \tag{7}$$

$$\Gamma_\omega = \mu + \frac{\pi_t}{\sigma_\omega} \tag{8}$$

The empirical constants of the SST model are presented in Table 2:

This study deals with heat transfer through the laminar regime convection between the steel shell and its external environment. It describes the movement of a fluid due to changes in density as a function of temperature. Thus, there is a coupling between the dynamic and the thermal. For all convection problems, the wall heat exchanges are measured by highlighting the value of the Nu number.

Since our study has an orientation towards heat transfer with the existence of a rectangular fin with a finite end, we give the equation that governs this phenomenon [41]:

$$\frac{d}{dx}\left(\lambda A \frac{dT}{dx}\right) - hp(T - T_\infty) = 0 \tag{9}$$

For heat transfer by natural convection, The Nusselt number correlation for the horizontal cylinder with plate fins (Nu) is given by [41,42]:

$$Nu = \left(1 - 0.117N + 0.353\left(\frac{H}{D}\right)\right)\left(0.6 + \frac{0.387Ra^{1/6}}{\left(1+(0.559/Pr)^{9/16}\right)^{8/27}}\right)^2 \tag{10}$$

The fin efficiency η, which is written as follows [41,42]:

$$\eta = \frac{(hp\lambda A_c)^{0.5}}{hA_f}\frac{\tanh\left(\sqrt{\frac{hp}{\lambda A_c}}l\right)+\left(h/\sqrt{\frac{hp}{\lambda A_c}}\lambda\right)}{1+\left(h/\sqrt{\frac{hp}{\lambda A_c}}\lambda\right)\tanh\left(\sqrt{\frac{hp}{\lambda A_c}}l\right)} \tag{11}$$

Mesh Optimization

The quality of the simulation results is closely linked to the model used, the mesh used and optimized. The choice of the model is subordinated to the type of information that we want to obtain from the simulation.

Table 3. Mesh parameter

Number of elements	Number of nodes
98678	100400
198145	210110
203011	301896

Validation

We validated our simulation results with a curve taken on-site in the control room of the cement plant. In this real case, all thermal, mechanical, and physico-chemical phenomena present in this type of equipment, as well as the state of the refractory brick, the state of the crust, and the actual thickness of the shell, are taken into account. In our simulation, we neglected certain parameters that we could not control. Despite this, the shapes of the curves (simulated and real) are similar, and the maximum error does not exceed 30% at a single point, while the average error is around 12%.

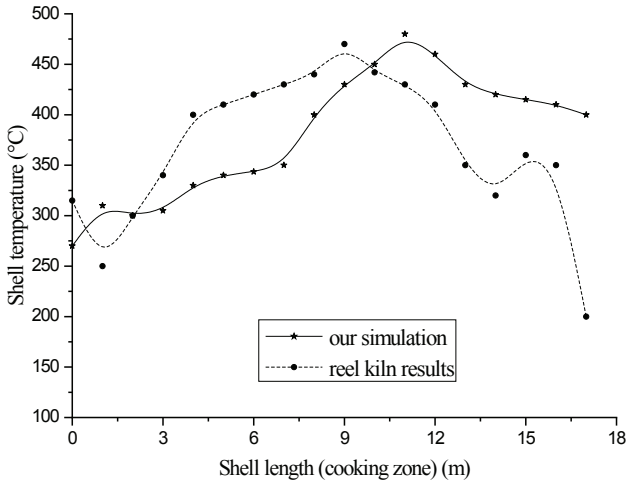

Figure 2. Distribution of the temperature outside the shell of the furnace (case of validation).

RESULTS AND DISCUSSION

Variation of the Hot Air Injection Velocity of the Burner

The purpose of this case study is to determine the effect of air injection velocity at the kiln burners on the thermal behavior of the shell. Five tests were carried out, this velocity was varied from 13.74 m/s to 53.74 m/s to deduce the maximum temperature value of the shell.

Figure 3 shows the evolution of temperature as a function of hot air velocity. We notice that as the air velocity increases, the outside temperature of the shell increases, which is logical, because a higher velocity leads to a hotter flame, which leads to an increase in the temperature. The temperature increases relatively with the increase in the velocity of injection of hot air from the burner. The temperature profiles have the same trend and the same shape, with a gradual increase up to the distance of 11 m, where the maximum temperature is found, then there is a slight decrease in this parameter. We also note that the velocity of the air injection has a moderate impact, since it is necessary to choose this velocity well in order to protect our shell from heating. It can also be seen that the maximum increase in temperature is 5% from one velocity value to another.

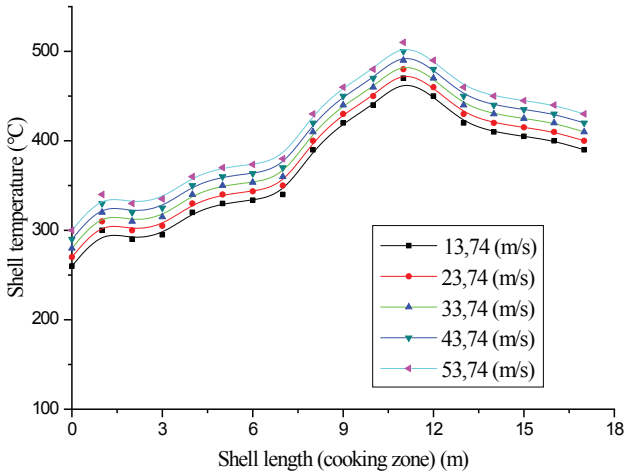

Figure 3. Evolution of the outer shell temperature as a function of the hot air velocity.

The Variation of the Internal Temperature of the Kiln

In this part, we wanted to know the effect of another parameter which is the variation of the hot air temperature of the burner inside the kiln. Figure 4 shows the variation in the outside temperature of the shell as a function of the hot air temperature inside the oven. The same rate is observed for each variation as well as a gradual increase in temperature up to the hottest point located at the 11 m length of the kiln. There is a decrease in the curve and a decrease in the temperature values.

The maximum values reach significant values, thus for the value of 1050°C of the air inside the kiln, we have an outside temperature of the shell of 416°C, while for the value of 1450°C, which is the operating temperature of a cement kiln, the external temperature reaches 496°C. This high temperature can damage the shell by plastic deformation.

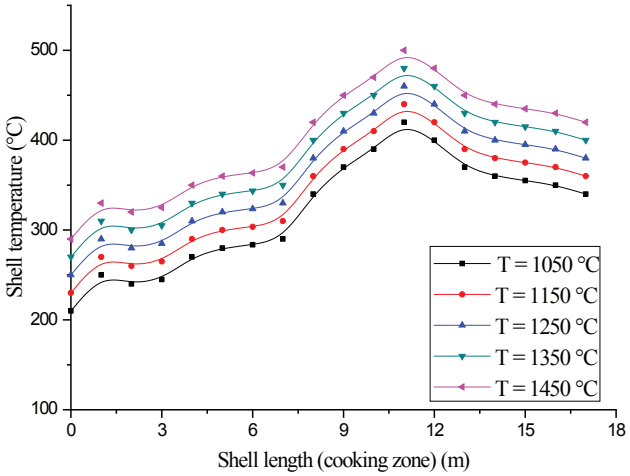

Figure 4. Outside temperature of the shell as a function of inside temperature of the furnace.

We note that we have a maximum variation of the temperature of 12%, this value has an important significance in the category of high temperatures and thus it is necessary to choose this parameter well during the operation of such industrial equipment, in order to to preserve.

Variation in Shell Temperature as a Function of Ambient Air Temperature

In this part, we wanted to know the effect of the variation of the ambient air injection temperature. Figure 5 represents the variation in the outside temperature of the shell as a function of the ambient air temperature. We observe the same shape as the previous curves, with a progression of the temperature up to the length of 11 m and then begins a decrease. We took 5 values of the ambient temperature from 5°C to 48°C and this according to the geographical location of our site and in relation to the different winter and summer seasons. It can be seen that this parameter does not have a significant impact, because the maximum variation does not exceed the value of 3%, i.e. a deference of 5°C (from 18°C to 28°C) in the temperature of the shell, which insignificant for such equipment whose temperature exceeds 1400°C. Note that the change in temperature from 5°C (winter) to 48°C (summer) may have an influence on the variation in the temperature outside the shell.

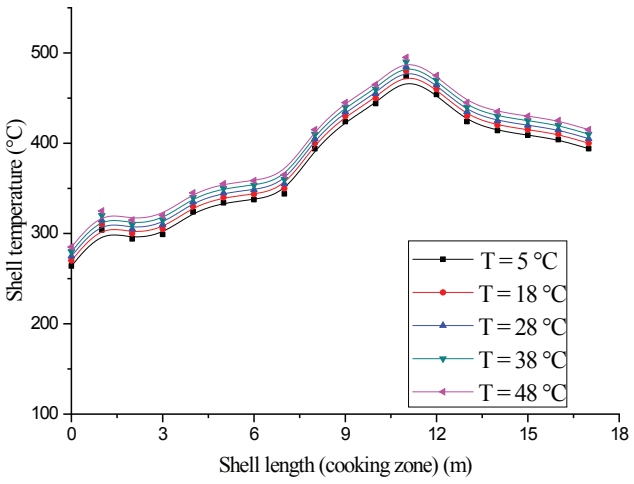

Figure 5. Outside temperature of the shell as a function of the ambient air temperature.

Shell Fitted with Fins

This second part of our study will be the same as the previous one, but modifying the geometry of the kiln in the cooking zone by adding rectangular fins. Figure 6 shows the new geometry of the shell of the rotary kiln studied. This zone is equipped with 72 fins, of 1 m length, 15 cm wide, and 15 cm high. These fins are spaced 1 m apart. Thus we will have 9 fins along the length and 8 on the circumference. For the simulation, we took the same boundary conditions as that of the smooth shell and in order to deduce the effect of these fins on the behavior of the temperature parameter of the shell.

The first part showed us that the temperature of the shell reaches values exceeding 500°C. At these temperatures, the shell steel reaches the plastic phase and the deformation will be permanent, which will cause problems for the installation of the refractory brick.

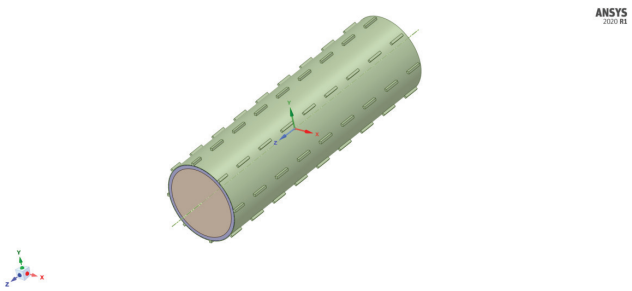

Figure 6. Cooking zone of the kiln with the 72 fins.

Comparison of Shell Temperatures with E Without Fins

The Figure 7 shows that the shell fitted with fins has a temperature gain of 32% compared to that without fins and 42% for that on site. The maximum temperature reached by the finned shell is 380°C, while that on site is 430°C and that without fins is 480°C.

It can be concluded that the insertion of the fins on the outer surface of the shell section which is the cooking zone, gives a considerable reduction in the temperature of the shell. This difference makes the oven work well and prolongs its life.

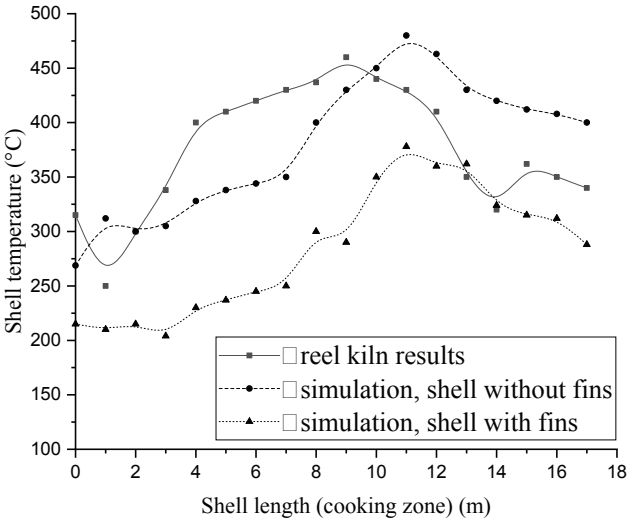

Figure 7. Comparison between the outside temperature of the shell with and without fins.

Table 4. The variation of the outside temperature of the shell as a function of the inside temperature of the kiln.

Temperature inside the kiln (°C)	1050	1150	1250	1350	1450
Shell temperature without fins (°C)	416	436	456	476	496
Shell temperature with fins (°C)	318	338	358	378	398
Difference (%)	23.6	22.5	21.5	20.6	19.8

The Variation of the Hot Air Temperature of the Burner

In this part, we wanted to know the effect of the variation of the hot air temperature of the burner. For this, we deduced the distribution of the external temperature of the shell with respect to the length of the kiln near the cooking zone. From Table 4 we can see that the reduction in the maximum temperature exceeds 20%, in the case of shell with fin than that without fin.

In Figure 8, the shapes of the curves are the same with a progressive increase, until reaching a maximum at the distance of 11 m, then decreases. The external temperature values of the shell fitted with fins are lower, with an overall reduction that can reach 40%. Similarly, the variation in the internal temperature of the kiln has a clear impact on the shell without fin, with an increase of approximately 11%, whereas it is approximately 12% in the case of the shell with fin.

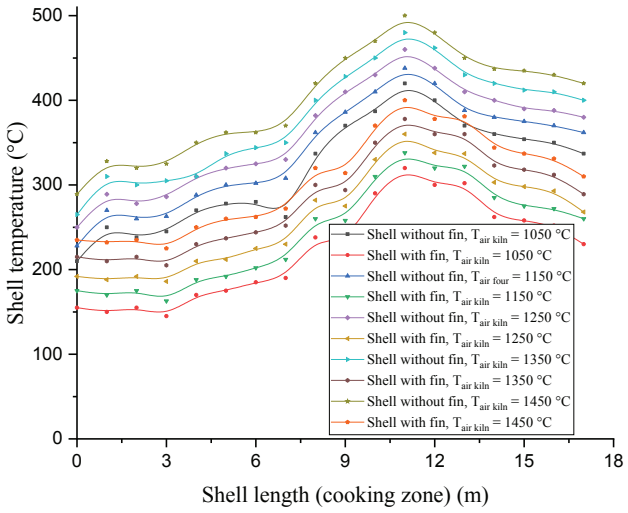

Figure 8. The variation in the outside temperature of the shell as a function of the inside temperature of the shell.

Variation of the Hot Air Injection Velocity of the Burner

Table 5 shows the simulation results of the maximum external temperature of the shell in the cooking zone for the two cases with and without fins. The increase in the air injection velocity of the burner causes an increase in temperature, this is the same for both cases. But we notice for the temperatures of the case without fins are more important than that with fins. Thus for the velocity of 13.75 m/s, we have a temperature of 470°C for the case without fins and 385°C for the case with fins, so a difference of 85°C (18%). This difference reaches its maximum at 20.6% for the velocity of 53.74 m/s. which will allow a greater flow of heat to be evacuated and protect our shell from hot spots.

In figure 9, we wanted to show the variation of the external temperature of the shell for the two cases with and without fins on the section of shell according to different hot air injection velocities. The temperature profiles have the same trend and the same appearance. This representation gives us a very clear idea of the efficiency of the fins installed on the external surface of the shell section of the cooking zone. The temperature reduction varies between 30% and exceeds 33%, which is very important for this type of industry. With a shell without fins, the maximum temperature reached is 510°C, while when the fins are installed it only reaches 405°C, therefore we have a reduction of 105°C.

Ambient Air Temperature Variation

Figure 10 shows the variation in the outside temperature of the shell as a function of the ambient air temperature. The representation is made for both cases, namely without and with fins. The curves have the same trend, an increasing progression up to a maximum at the distance of 11 m, then a decrease. With regard to the effect of ambient temperature, it can be seen that its effect is minimal, since the curves are very close. We notice a very clear difference between the curves with fins and those without fins. The maximum temperature is 390°C for the finned case, while

Tableau 5. Maximum shell temperature as a function of hot air injection velocity

Vitesse d'air chaud (m/s)	13.74	23.74	33.74	43.74	53.74
Température de la virole sans ailettes (°C)	470	480	490	500	510
Température de la virole avec ailettes (°C)	385	390	395	400	405
Difference (%)	18	18.75	19.4	20	20.6

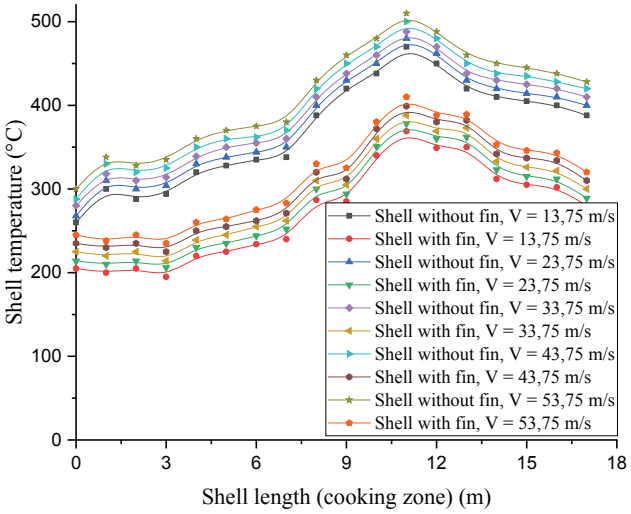

Figure 9. The external temperature of the shell with fins as a function of the hot air velocity.

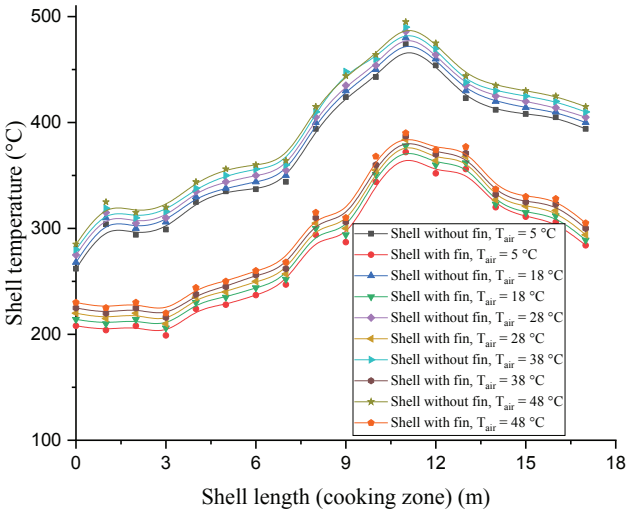

Figure 10. Shell temperature variation as a function of ambient air temperature.

it is 495°C for the finless case, so there is a reduction of 105°C, which is very interesting for the protection of this equipment.

CONCLUSION

The main purpose of our work is to highlight the impact of the cooling of the shell of a rotary kiln in the cooking zone over a length of 17 m, which is thermally stressed. We chose cooling by the use of fins, which is an innovative solution installed on the rotary kiln.

The integration of fins on the external surface of the shell has given us very interesting results, since the reduction of the external temperature reaches values of more than 40%. This has a considerable impact on the protection of the ferrule.

We also wanted to see the impact of some factors such as the hot air injection velocity, the internal air temperature of the kiln and the ambient temperature on the development of the temperature of the shell. Thus, it could be deduced that the velocity of hot air injection has a considerable effect on the behavior of the external temperature of the shell. We noticed an increase in temperature during the transition from one value to another of the air inside the kiln, until reaching its maximum at T= 1450°C. This observation is the same for the two cases where the shells was with or without fins, while the comparison of the two leads to a reduction in the external temperature of the shell of approximately 40% at most. For the third parameter, which is the ambient temperature, we see that its effect is very small and does not exceed 3%. But when changing from the simple shell to a shell with fin, the reduction in temperature is significant and reaches the value of 33%.

This study allowed us to determine a way to reduce the outside temperature of the shell in the hottest part of the kiln, namely the cooking zone. Thus, the cooling of a shell of a cement rotary kiln was numerically simulated by the insertion of 72 fins on the external surface of the shell.

As a perspective to this work, we opt for an optimization in the shape and dimensions of the fins. As well as the transition from a numerical to an experimental study that can identify the more global problem.

NOMENCLATURE

Nu	Nusselt number
h	Heat transfer coefficient, W/m²°C
p	Fin perimeter, m
D	Cylinder diameter, m
A	Area, m²
A_c	Fin cross-sectional area, m²
A_f	Fin surface area, m²
η	Fin efficiency
N	Fins number
g	Gravitational acceleration, m/s²
H	Fin height, m
L	Fin length, m
t	Fin thickness, m
Pr	Prandt number
Ra	Rayleigh number
U, U’	Mean velocity in tensor notation
P	Pressure
μ	Dynamic viscosity, kg/m.s
λ	Thermal conductivity, W/m.°C
T	Temperature
ρ	Density of the fluid, kg/m³
C_p	Specific heat, J/kg.K
S_Φ	Local production of ϕ.
Φ	Generalized variable
Γ	Coefficient of diffusion

Γ	Effective diffusivity
η	Efficiency
S_Φ	Local production of ϕ.
ω	Specific dissipation rate
G_k	Term of production of k
$G\omega$	Term of production of ω
S_k	Mean strain rate tensor
σ	Normal viscous stress, N/m^2
α	Thermal diffusivity ($\lambda/\rho C_p$)

indice

i, j	Indices according to the axes
‘	Fluctuation index

AUTHORSHIP CONTRIBUTIONS

Authors equally contributed to this work.

DATA AVAILABILITY STATEMENT

The authors confirm that the data that supports the findings of this study are available within the article. Raw data that support the finding of this study are available from the corresponding author, upon reasonable request.

CONFLICT OF INTEREST

The author declared no potential conflicts of interest with respect to the research, authorship, and/or publication of this article.

ETHICS

There are no ethical issues with the publication of this manuscript.

REFERENCE

[1] Bouhafs M, Meghdir A, Adjeloua A, Ameur H. Numerical simulation of the fin impact on the cooling of the shell of a rotary kiln. J Adv Res Fluid Mech Therm Sci 2023;103:68−84. [CrossRef]

[2] Shvachko DG, Shcherbina VY, Borshchik SA. Thermal protection insulation in the lining of the rotary kilns. Mod Engineer Innov Technol 2021;16:18−23.

[3] Gallo A, Alonso E, Perez-Rabago C, Fuentealba E, Roldanb MI. A lab-scale rotary kiln for thermal treatment of particulate materials under high concentrated solar radiation: Experimental assessment and transient numerical modeling. Sol Energy 2019;188:1013−1030. [CrossRef]

[4] Wirtz S, Pieper C, Buss F, Schiemann M, Schaefer S, Scherer V. Impact of coating layers in rotary cement kilns: Numerical investigation with a blocked-off region approach for radiation and momentum. Therm Sci Engineer Prog 2020;15:100429. [CrossRef]

[5] Rindang A, Panggabean S, Wulandari F. CFD Analysis of temperature drying chamber at rotary dryer with combined energy. IOP Conf Ser J Phys Conf Ser 2019;1155:012037. [CrossRef]

[6] Gu C, Yuan Z, Sun S, Guan L, Wu K. Simulation investigation of drying characteristics of wet filamentous biomass particles in a rotary kiln. Fuel Process Technol 2018;178:344−352. [CrossRef]

[7] Bongo Njeng AS, Vitu S, Clausse M, Dirion JL, Debacq M. Wall-to-solid heat transfer coefficient in flighted rotary kilns: Experimental determination and modeling. Exp Therm Fluid Sci 2018;91:197−213. [CrossRef]

[8] Mirhosseini M, Rezaniakolaei A, Rosendahl IL. Numerical study on heat transfer to an arc absorber designed for a waste heat recovery system around a cement kiln. Energies 2018;11:671. [CrossRef]

[9] Wang K, Li J, Wang P, Cheng L. Experimental and numerical studies on the air-side flow and heat transfer characteristics of a novel heat exchanger. Appl Therm Engineer 2017;123:830−844. [CrossRef]

[10] Yin Q, Du WJ, Ji XL, Cheng L. Optimization design based on the thermal resistance analyses of heat recovery systems for rotary kilns. Appl Therm Engineer 2017;112:1260−1270. [CrossRef]

[11] Ramanenka D, Antti ML, Gustafsson G, Jonsén P. Characterization of high-alumina refractory bricks and modeling of hot rotary kiln behavior. Eng Fail Anal 2017;79:852−864. [CrossRef]

[12] Yin Q, Du WJ, Cheng L. Optimization design of heat recovery systems on rotary kilns using genetic algorithms. Appl Energy 2017;202:153−168. [CrossRef]

[13] Agrawal A, Ghoshdastidar PS. Numerical simulation of heat transfer during production of rutile titanium dioxide in a rotary kiln. Int J Heat Mass Transf 2017;106:263−279. [CrossRef]

[14] Csernyei CM. Numerical modelling of a rotary cement kiln with external shell cooling fans. Electronic Thesis and Dissertation Repository; 2016. [CrossRef]

[15] Yin Q, Chen Q, Du WJ, Ji XL, Cheng L. Design requirements and performance optimization of waste heat recovery systems for rotary kilns. Int J Heat Mass Transf 2016;93:1−8. [CrossRef]

[16] Shahin H, Hassanpour S, Saboonchi A. Thermal energy analysis of a lime production process: Rotary kiln, preheater and cooler. Energy Conver Manage 2016;114:110−121. [CrossRef]

[17] Ustaoglu A, Alptekin M, Akay ME. Thermal and exergetic approach to wet type rotary kiln process and evaluation of waste heat powered ORC (organic Rankine cycle). Appl Therm Engineer 2016;112:281−295. [CrossRef]

[18] Csernyei CM. Numerical modelling of a rotary cement kiln with external shell cooling fans. A thesis submitted in partial fulfillment of the requirements

for the degree in Master of Engineering Science, Graduate Program in Mechanical and Materials Engineering, The University of Western Ontario; 2016. [CrossRef]
[19] Liu H, Yin H, Zhang M, Xie M, Xi X. Numerical simulation of particle motion and heat transfer in a rotary kiln. Powder Technol 2016;287:239−247. [CrossRef]
[20] Goshayeshi HR, Poor FK. Modeling of rotary kiln in cement industry. Energy Power Engineer 2016;8:23−33. [CrossRef]
[21] Gaurav GK, Khanam S. Analysis of temperature profile and % metallization in rotary kiln of sponge iron process through CFD. J Taiwan Inst Chem Engineer 2016;63:473−481. [CrossRef]
[22] Csernyei CM, Straatman AG. Forced convective heat transfer on a horizontal circular cylinder due to multiple impinging circular jets. Appl Therm Engineer 2016;105:290−303. [CrossRef]
[23] Goshayeshi HR, Poor FK. Modeling of rotary kiln in cement industry. Energy Power Engineer 2016;8:23−33. [CrossRef]
[24] Moussi K, Touil D, Fedailaine M, Belaadi S. Modèle d'échange d'énergie et de matière dans un four rotatif, incluant la combustion. Rev Energ Renouv 2015;18:143−152. [French] [CrossRef]
[25] Luo Q, Li P, Cai L, Zhou P, Tang D, Zhai P, et al. A thermoelectric waste-heat-recovery system for portland cement rotary kilns. J Electron Mater 2015;44:1750−1762. [CrossRef]
[26] Atmaca A, Yumrutas R. Analysis of the parameters affecting energy consumption of a rotary kiln in cement industry. Appl Therm Engineer 2014;66:435−444. [CrossRef]
[27] Ariyaratne WKH, Malagalage A, Melaaen MC, Tokheim L. CFD modeling of meat and bone meal combustion in a rotary cement kiln. Int J Model Optim 2014;4:263−272. [CrossRef]
[28] Yi Z, Xiao H, Song J, Guangbai A, Zhou J. Mathematic simulation of heat transfer and operating optimization in alumina rotary kiln. J Cent South Univ 2013;20:2775−2780. [CrossRef]
[29] Caputo AC, Pelagagge PM, Salini P. Performance modeling of radiant heat recovery exchangers for rotary kilns. Appl Therm Engineer 2011;31:2578. [CrossRef]
[30] Paramane SB, Sharma A. Heat and fluid flow across a rotating cylinder dissipating uniform heat flux in 2D laminar flow regime. Int J Heat Mass Transf 2010;53:4672−4683. [CrossRef]
[31] Larsson IAS, Lindmark EM, Lundstrom TS, Marjavaara D, Toyra S. Kiln aerodynamics: Visualisation of merging flow by usage of PIV and CFD. Seventh International Conference on Computational Fluid Dynamics in Minerals and Process Industries: CSIRO; Melbourne, Australia, 2009.
[32] Krishnayatra G, Tokas S, Kumar R, Zunaid M. Parametric study of natural convection showing effects of geometry, number and orientation of fins on a finned tube system: A numerical approach. J Therm Engineer 2022;2:268−285. [CrossRef]
[33] Rout SK, Hussein AK, Mohanty CP. Multi-objective optimization of a three-dimensional internally finned tube based on response surface methodology (RSM). J Therm Engineer 2015;2:131−142. [CrossRef]
[34] Bano T, Ali HM. An overview of recent progress in condensation heat transfer enhancement across horizontal tubes and the tube bundle. J Therm Engineer 2021;1:1−36. [CrossRef]
[35] Mohamad S, Rout SK, Senapati JR, Sarangi SK. Entropy generation analysis and cooling time estimation of a blast furnace in natural convection environment. Numer Heat Transf Part A Appl 2022;82:666−681. [CrossRef]
[36] Mohamad S, Senapati JR, Routh SK, Sarangi SK. RETRACTED: Development of Nusselt number correlation in natural convection over the walls of a blast furnace: A CFD approach. Proc Inst Mech Engineer Part E J Process Mech Eng 2021.
[37] Rout SK, Mishra DP, Nath Thatoi D, Acharya AK. Numerical analysis of mixed convection through an internally finned tube. Adv Mech Engineer 2012;4:918342. [CrossRef]
[38] Mebarek-Oudina F, Laouira H, Hussein AK, Omri M, Abderrahmane A, Kolsi L, et al. Mixed convection inside a duct with an open trapezoidal cavity equipped with two discrete heat sources and moving walls. Mathematics 2022;10:929. [CrossRef]
[39] Patankar SV. Numerical Heat Transfer and Fluid Flow. New York: McGraw Hill; 1980.
[40] Menter FR. Zonal two equation k-ω turbulence models for aerodynamic flows. AIAA Paper 93-2906; 1993. [CrossRef]
[41] Incropera FP, Dewitt DP, Bergman TL, Lavine AS. Fundamentals of Heat and Mass Transfer. 6th ed. New York, NY: John Wiley & Sons; 2007.
[42] Kim HJ, An BH, Park J, Kim DK. Experimental study on natural convection heat transfer from horizontal cylinders with longitudinal plate fins. J Mech Sci Technol 2013;27:593−599. [CrossRef]